

Evaluation of Heat and Mass Transfer Efficiency of Milk Spray Drying by Computational Simulation Tool

Pham Van Khanh, Tran Thi Thu Hang*

School of Heat Engineering and Refrigeration Engineering, Hanoi University of Science and Technology, Hanoi, Vietnam

*Corresponding Author Email: hang.tranthithu@hust.edu.vn

ABSTRACT: A spray drying model is simulated by the computational fluid dynamics (CFD). By changing the input conditions, the temperature and velocity fields in the drying chamber are examined and the volumetric heat transfer coefficient in each condition is calculated. It is obtained that the increase in the inlet air temperature and the air flow rate makes the decrease in the average volumetric heat transfer coefficient because of the increase in the energy loss; besides, particle residence time is shorter at the higher inlet air flow rate.

KEYWORDS: CFD, spray drying, volumetric heat transfer, milk.

INTRODUCTION

Spray drying is a drying process in which a drying material in a liquid form is fast dried into a powder product [1]. Currently, the spray drying method has been widely applied in industries like food, medicine, materials, etc.[2] There are many high quality products of spray drying process such as milk powder, tea, coffee, vitamins, enzymes, drugs antibiotics, paint colors, ceramic materials, etc. Spray drying is a very complex process in terms of heat, mass and momentum transfers. There are many parameters that affect on process and product quality, not only operational conditions like air temperature, feed flow rate, or the way of phase mixing (co-current or counter-current), but also parameters that depend on dryer geometry like hydrodynamics of continuous-phase flow [3]. To minimize operating costs, spray-drying systems need to be optimized in terms of energy consumption and physical properties of the product. Computational fluid dynamic (CFD) is an effective tool for this optimization because this allows to simulate the real object [4][5][6]. Besides, CFD model gives the accurate prediction changes of air flow parameters and heat and mass transfer of multiphase so it can be applied to determine the effect of operating condition and the dryer geometry on both product quality and energy consumption [7].

Typically, to design one dryer, it is necessary to determine the quantity of average volumetric heat transfer coefficient, α_V [8][9]. Because this coefficient represents for the heat and mass transfer efficient in whole dryer and it allows to calculate dryer dimensions. For several dryers, α_V is almost determined by experiments while the extrapolation of this coefficient to cases, drying conditions outside the experimental conditions is inconclusive . But if we apply the CFD theoretical model over a wide range of drying conditions to find this coefficient, the applicability can be extended for different cases. Besides, residence time of particles have much more impact on the product quality [10]; thus, in this work, particle residence time and volumetric heat transfer coefficient are examined under different operating conditions.

METHODOLOGY

Configuration of the spray dryer

Figure 1 shows a co-current spray dryer with the dimensions of $h \times d = 6.1 \text{ m} \times 0.4 \text{ m}$. Hot air and sprayed solution flow from the top to the bottom of dryer. The tower is insulated partly from the top of the tower to the height of 0.8 m from the bottom. The average heat transfer coefficient from outside wall to the air for the insulated part and non-insulated part are $4.3 \text{ W/m}^2\text{K}$ and $7.1 \text{ W/m}^2\text{K}$ respectively.

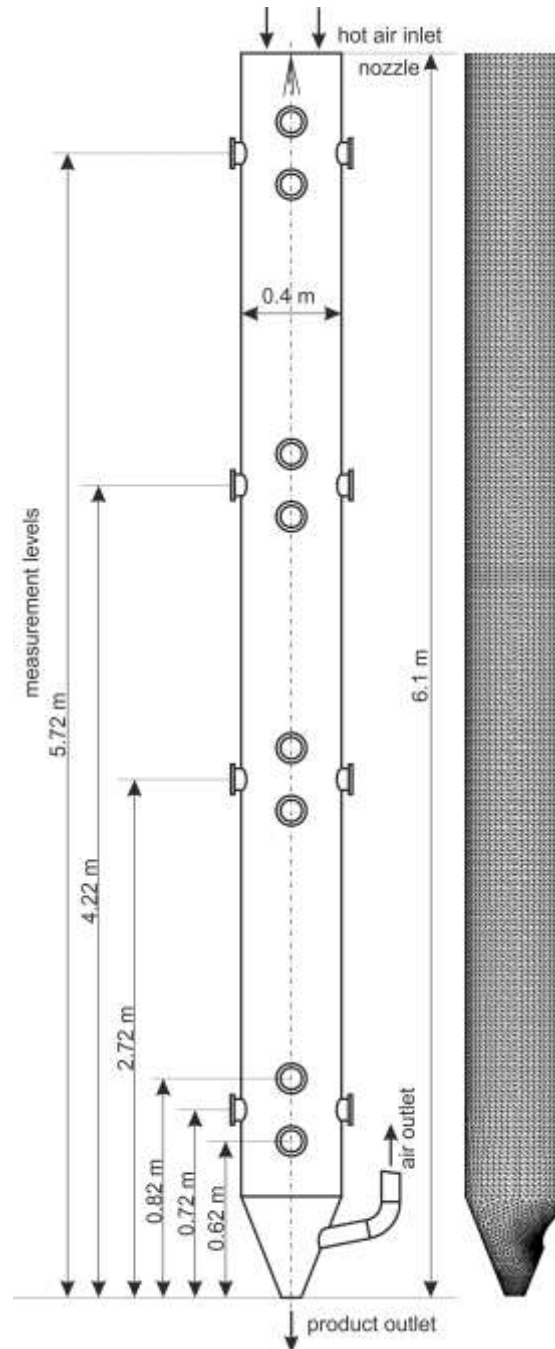


Figure 1. Geometry of spray dryer [3]

Meshing and setup

Mesh is generated with 385,000 tetrahedral elements as Fig.1, in which a five-step boundary layer is applied for the area near the wall. The quality mesh is evaluated by several indexes as: skewness is 0.88, aspect ratio is 5.53. Several various mesh size and element shape were tested to yield grid-independent solution. Simulation setup for skim milk spray drying with the initial conditions as: solid mass fraction of 30%, particle velocity of 20 m/s, feed

temperature of 30°C, feed flow rate of 0.0025 kg/s. The inlet air flow rate and inlet air temperature are changed to from 0.06 kg/s to 0.15 kg/s and 140°C to 200°C respectively to check effects of these parameters on the heat and mass transfer efficiency.

The Euler-Lagrange approach is applied to couple computation fluid dynamic and discrete phase model. In which, fluid phase is continuous phase and transport phenomena are described by Navier-Stokes equations while the discrete phase is concerned by tracking a large number of particles. The turbulent fluid phase is treated by standard $k - \varepsilon$ model. Boundary condition used for inlet air is inlet mass flow rate while the outlet is outflow condition. The chamber wall is setup as wall with convective heat transfer conditions in which the heat transfer coefficients are 4.3 W/m²K for the insulated area and 7.1 W/m²K for uninsulated area.

Evaporation model

The particle mass m is the sum of the masses of the components [11]:

$$m = \sum m_i \quad (1)$$

The density of the particle ρ_p can be either constant, or volume-averaged :

$$\rho_p = \left(\sum \frac{m_i}{m\rho_i} \right)^{-1} \quad (2)$$

Equation of heat balance for particle and air in the drying chamber:

$$m_p c_p \left(\frac{dT_p}{dt} \right) = A_p \varepsilon_p \sigma (\theta_R^4 - T_p^4) + h A_p (T_\infty - T_p) + \sum \frac{dm_i}{dt} (h_{i,p} - h_{i,g}) \quad (3)$$

The equation for the particle temperature T consists of terms for radiation, convective heat transfer and vaporization. Radiation heat transfer to the particle equal zero. The mass of the particle components m_i is only influenced by the vaporization, where $M_{w,i}$ is the molecular weight of species i .

The vapor flux is determined by equation:

$$\frac{dm_i}{dt} = A_p M_{w,i} k_{c,i} (C_{i,s} - C_{i,\infty}) \quad (4)$$

The mass transfer coefficient $k_{c,i}$ of component i is calculated from the Sherwood correlation [11].

$$Sh_{AB} = \frac{k_c d_p}{D_{i,m}} = 2.0 + 0.6 Re_d^{1/2} Sc^{1/3} \quad (5)$$

Where $D_{i,m}$ is diffusion coefficient of vapor in the bulk (m²/s)

$$Sc = \frac{\mu}{\rho D_{i,m}} \text{ is the Schmidt number}$$

d_p is particle diameter (m)

The concentration of vapor at the particle surface $C_{i,s}$ depends on the saturation pressure of the component.

$$C_{i,s} = \frac{P_{sat}(T_p)}{RT_p} \quad (6)$$

Where R is the universal gas constant.

The concentration of vapor in the bulk gas is known from solution of the transport equation for species i for nonpremixed or partially premixed combustion calculations:

$$C_{i,\infty} = X_i \frac{p}{RT_\infty}$$

Where X_i is the local bulk mole fraction of species i , p is the local absolute pressure, and T_∞ is the local bulk temperature in the gas.

The heat transfer coefficient, h , is evaluated using the correlation of Ranz and Marshall:

$$Nu = \frac{hd_p}{k_\infty} = 2.0 + 0.6Re_d^{1/2} Pr^{1/3} \quad (7)$$

Where

d_p = particle diameter (m)

k_∞ = thermal conductivity of the continuous phase (W/m-K)

Re_d = Reynolds number based on the particle diameter and the relative velocity

Pr = Prandtl number of the continuous phase ($c_p\mu/k_\infty$)

Volumetric heat transfer coefficient

The mean heat transfer coefficient, α_v represents for heat transfer efficiency in the whole drying chamber. This is also the parameter to calculate dryer volume. α_v is calculated by:

$$\alpha_v = \frac{Q}{V \cdot \overline{\Delta t}} \quad (8)$$

In which, Q is the total energy transferred between particles and continuous phase in the chamber, $\overline{\Delta t}$ is obtained from average of difference between particle temperature and gas temperature at all cells in the chamber.

SIMULATION RESULTS

Simulations are implemented for various inlet air temperature and air velocity. Results are shown in two sections as following

Effects of inlet air temperature

Temperature fields in the drying chamber at different inlet air temperatures are illustrated in Fig.2. In each case, from the top to the bottom of dryer, three different areas can be observed as following: area near air inlet is the highest temperature area, temperature near the center is low; after that temperature in the center region drops dramatically due to the evaporation of particle; finally, air temperature is almost uniform in the center area but is low near the wall due to heat transfer to the wall.

It is also obtained that the more intense and earlier evaporation occurs at higher inlet air temperature. Besides, at higher inlet air temperature the area with higher temperature is wider than that at lower inlet air temperature. For all cases, at the end of drying chamber the temperature is uniform; however, the exhaust air in case of hot inlet air is also hot.

Table 1 shows the particle residence time and average volumetric heat transfer coefficient and Fig. 3 presents the detailed effect of inlet air temperature on α_v . The increase in the inlet air temperature makes the mean particle residence time decrease. This can be explained by the reduction of air density when temperature raises, results in the increase of air velocity so the particles are flowed faster. The lower air temperature gives the higher volumetric heat transfer coefficient because the difference of air and particle temperatures reduces at lower inlet air temperature. It can be concluded that in this case, the increase in the inlet air temperature does not enhance the heat and mass transfer but make more wasted energy.

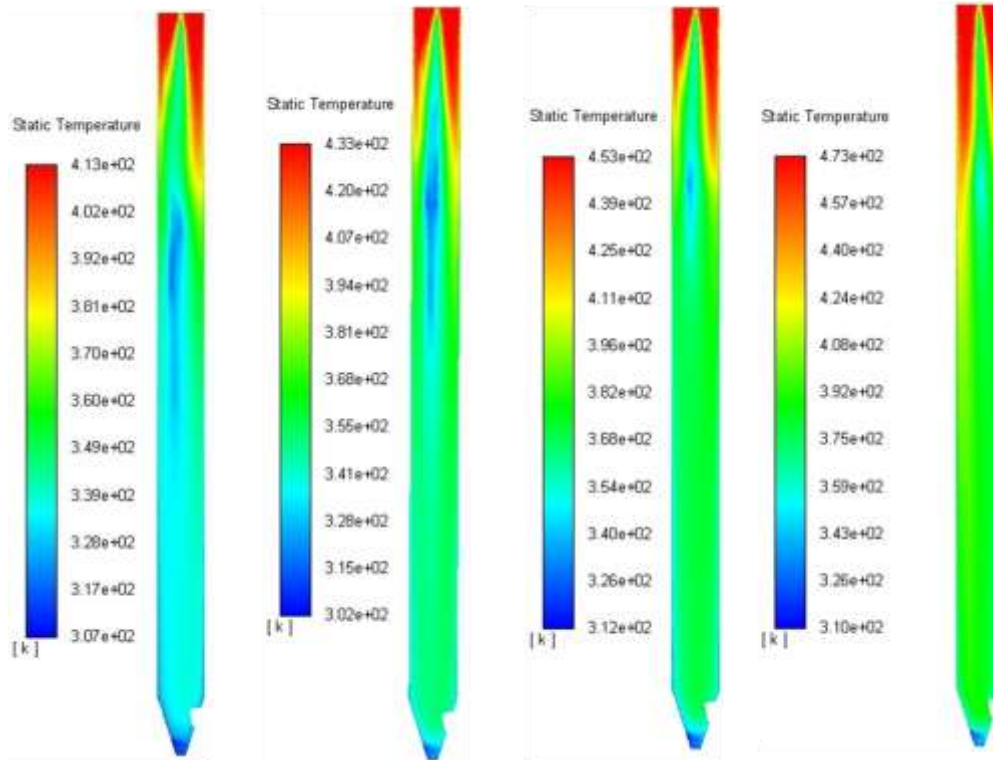


Figure 2. Changes in air temperature profile along the spray tower obtained from CFD simulations for the initial air mass flow rate $G_g = 0.075$ kg/s.

Table 1. Impacts of initial air temperature

$G_g = 0.075, \text{ kg/s}$					
$T_g, \text{ }^\circ\text{C}$	$\overline{\Delta t}, \text{ }^\circ\text{C}$	$V, \text{ m}^3$	$Q, \text{ W}$	$\alpha_v, \text{ W/m}^3\text{K}$	Time, s
200	16.93847	0.73374	4382	352.5786	2.92
180	14.19443	0.73374	4365.625	419.1662	3.15
160	13.43	0.73374	4344.615	440.8929	3.55

140	11.694	0.73374	4322.96	503.8206	4.06
-----	--------	---------	---------	----------	------

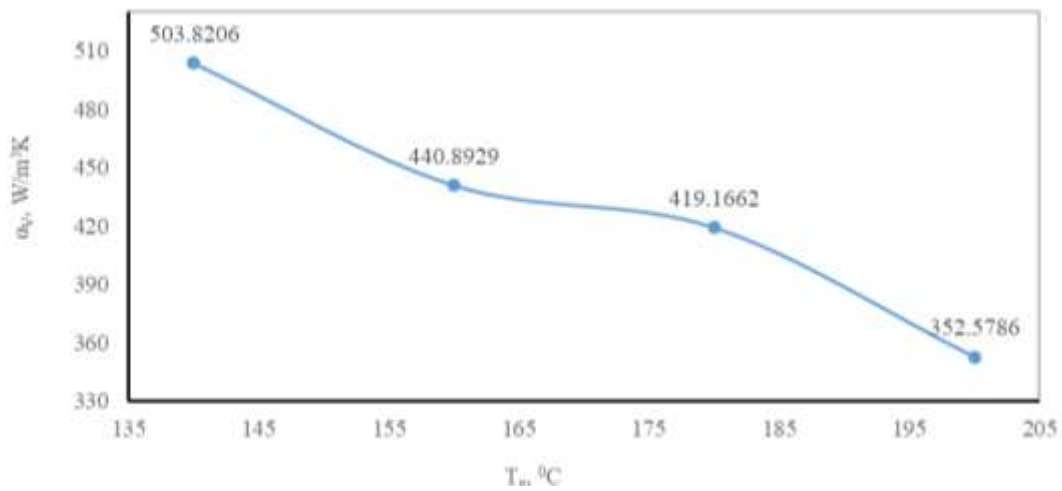


Figure 3. Change of volumetric heat transfer at various inlet air temperature ($G_g = 0.075$ kg/s)

Effect of initial air mass flow rate

To evaluate the effects of initial air mass flow rate, other operating conditions are kept constant, temperature fields inside the drying tower are shown in Fig. 4. It can be seen that along the chamber, there are three different areas which are similar to discussion in the section 3.1. The temperature fields in all cases are different: the greater the inlet air mass flow rate is, the wider the area with higher temperature has and the lower the area with high temperature difference has. Because the same latent heat used for evaporation process at the same feed flow rate, but the larger air mass flow rate gives more heat supplied for the evaporation so the higher air flow rate yields the less reduction in the air temperature. This results in the higher exhaust air temperature is obtained at higher air flow rate.

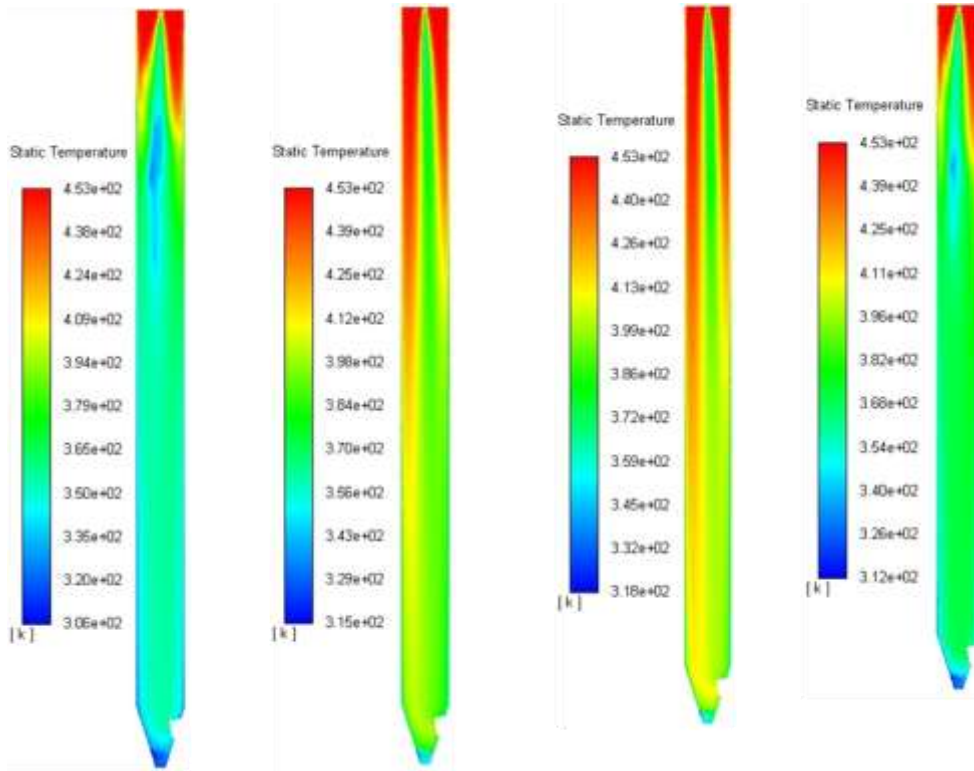


Figure 4. Changes in air temperature profile along the spray tower obtained from CFD simulations for the initial air temperature $T_g = 180$ °C.

Table 2. The affection of initial air mass flow rate condition

$T_g = 180, \text{ }^\circ\text{C}$					
$G_g, \text{ kg/s}$	$\overline{\Delta t}, \text{ }^\circ\text{C}$	$V, \text{ m}^3$	$Q, \text{ W}$	$\alpha_v, \text{ W/m}^3\text{K}$	Time, s
0.06	13.15367	0.73374	4346.503	450.3507	4.49
0.075	14.19443	0.73374	4365.625	419.1662	3.15
0.12	18.9626	0.73374	4398.953	316.1617	2.04
0.15	21.58165	0.73374	4412.33	278.6385	1.68

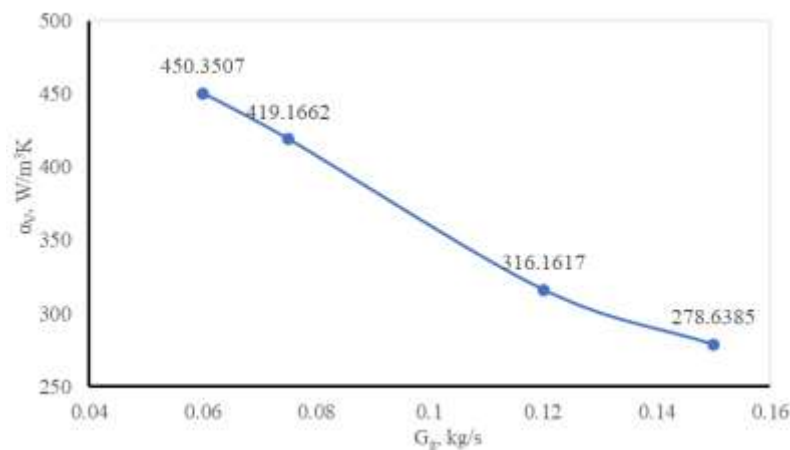


Figure 5. Effect of initial air mass flow rate on volumetric heat transfer coefficient ($T_g = 180^\circ\text{C}$)

Table 2 presents the change of average particle residence time and volumetric heat transfer coefficient. Particle residence time reduces when air mass flow rate increases due to the increase in the air velocity. Besides, the increase in the mass flow rate does not bring the increase in heat and mass transfer but decrease in the α_v which is shown more detailed in Fig. 5. This is because after as above discussion, the air temperature in the whole chamber increases at higher air mass flow rate. Thus, the more energy consumption supplied to the more air flow rate has no mean in the heat and mass transfer.

CONCLUSIONS

In this work, simulation results for spray drying of skim milk solution are presented for different initial air flow rate and temperature. It is concluded that the increase in the inlet air temperature and in the mass flow rate makes the early evaporation and the reduction in the particle residence time and volumetric heat transfer coefficient. For this spray drying system, these changes in operating conditions only wastes more energy by higher exaused air temperature.

With the final aim is optimization in spray drying process, other operating conditions should be checked to optimize in respect of minimum energy consumption and high product quality.

REFERENCES

- [1] T. T. H. Tran, J. G. Avila-Acevedo, and E. Tsotsas, "Enhanced methods for experimental investigation of single droplet drying kinetics and application to lactose/water," *Dry. Technol.*, vol. 34, no. 10, pp. 1185–1195, 2016.
- [2] M. Selvamuthukumar, *Handbook on Spray Drying Applications for Food Industries*. CRC Press, 2019.
- [3] M. Jaskulski, T. T. H. Tran, and E. Tsotsas, "Design study of printer nozzle spray dryer by computational fluid dynamics modeling," *Dry. Technol.*, 2019.
- [4] D. Aydin, S. E. Ezenwali, M. Y. Alibar, and X. Chen, "Novel modular mixed-mode dryer for enhanced solar energy utilization in agricultural crop drying applications," *Energy Sources, Part A Recover. Util. Environ. Eff.*, pp. 1–17, 2019.
- [5] S. Murugavelh, B. Anand, K. Midhun Prasad, R. Nagarajan, and S. Azariah Pravin Kumar, "Exergy analysis and kinetic study of tomato waste drying in a mixed mode solar tunnel dryer," *Energy Sources, Part A Recover. Util. Environ. Eff.*, pp. 1–17, 2019.
- [6] A. K. Babu, G. Kumaresan, V. Antony Aroul Raj, and R. Velraj, "CFD studies on different configurations of drying chamber for thin-layer drying of leaves," *Energy Sources, Part A Recover. Util. Environ. Eff.*, vol. 42, no. 18, pp. 2227–2239, 2020.

- [7] T. A. G. Langrish and D. F. Fletcher, "Prospects for the modelling and design of spray dryers in the 21st century," *Dry. Technol.*, vol. 21, no. 2, pp. 197–215, 2003.
- [8] T. Poós and V. Szabó, "Volumetric Heat Transfer Coefficient in Fluidized- Bed Dryers," *Chem. Eng. Technol.*, vol. 41, no. 3, pp. 628–636, 2018.
- [9] P. I. Alvarez and C. Shene, "Experimental determination of volumetric heat transfer coefficient in a rotary dryer," *Dry. Technol.*, vol. 12, no. 7, pp. 1605–1627, 1994.
- [10] M. Jaskulski, J. C. Atuonwu, T. T. H. Tran, A. G. F. Stapley, and E. Tsotsas, "Predictive CFD modeling of whey protein denaturation in skim milk spray drying powder production," *Adv. Powder Technol.*, vol. 28, no. 12, pp. 3140–3147, 2017.
- [11] ANSYS Inc, "Theory guide," 2017.